Multidim Syst Sign Process (2012) 23:515–524
DOI 10.1007/s11045-012-0177-4

COMMUNICATION BRIEF

A computerized system of nail-fold capillaroscopy for dry eye disease diagnosis

Mark C. Hou · Sheng-Chieh Huang · Hui-Min Wang · Cheng-Lung Tseng · Lun-Chien Lo · Ying-Ling Chen

Received: 15 February 2011 / Revised: 13 January 2012 / Accepted: 28 January 2012 /
Published online: 26 February 2012

Abstract Nail-fold Capillaroscopy is a convenient and non-invasive tool to evaluate peripheral circulation. Rheumatic diseases such as Raynaud's disease and systemic sclerosis are investigated mostly by nail-fold capillaroscopy. However, it has not been used popularly due to the lack of golden standard in both measurement procedure and objective quantity analysis. This study proposes a computerized system of nail-fold capillaroscopy (CNC). CNC includes standard measurement procedures and three criterions of microcirculation which are capillary density, capillary width and blood flow velocity. CNC is applied to the images of 36 normal subjects and seven patients of dry eye disease (DED). We found density and width of afferent capillary were the better parameters to identify DED ($p < 0.05$). CNC could be a good auxiliary diagnostic tool for DED.

This work has been presented at International Conference of Inflammation, Cardiometabolic Diseases and Cancer (ICICDC) 2010 in Taiwan.

M. C. Hou · S.-C. Huang · H.-M. Wang · C.-L. Tseng
sense/tcm SOC Lab, Department of Electrical Engineering, National Chiao Tung University,
1001 University Road, Hsinchu 300, Taiwan

M. C. Hou
e-mail: dr.markhou@gmail.com

S.-C. Huang
e-mail: schuang@cn.nctu.edu.tw

H.-M. Wang
e-mail: marcel.wang@gmail.com

C.-L. Tseng
e-mail: blake.ltseng@gmail.com

M. C. Hou · L.-C. Lo · Y.-L. Chen
Department of Chinese Medicine, Changhua Christian Hospital, 135 Nan-Siao Street,
Changhua 500-06, Taiwan

Y.-L. Chen (✉)
Graduate Institute of Education, National Changhua University of Education,
No. 1 Jin-De Road, Changhua 50006, Taiwan
e-mail: 139423@cch.org.tw

Keywords Nail-fold capillaroscopy · Image processing · Dry eye disease

1 Introduction

Nail-fold capillaroscopy is a non-invasive and easy to use tool for evaluating the microcirculation. In the human body, only mucosa, skin and sublingual capillaries can be observed directly by a microscope. The capillaries of nail-folds are arranged parallel to the skin which are perfectly good for visualization through a microscope with a video camera (Fagrell et al. 1977). Rheumatic diseases such as Raynaud's disease and systemic sclerosis are investigated frequently by nail-fold capillaroscopy (Grassi and Angelis 2007). Recently nail-fold capillaroscopy has been applied to diseases other than rheumatism for example diabetes, hypertension, acromegaly, and psoriasis (Gallucci et al. 2008). In severe diabetes, the capillaroscopy show dilated capillaries. In arterial hypertension, a reduced capillary density has been observed in patients and in preclinical stages. A reduction of nail-fold capillaries has also been observed in essential hypertension (Lambova and Müller-Ladner 2009; Antonios et al. 1999).

Dry eye disease (DED) is one of the most common disorders in ophthalmology. The estimated prevalence of DED is between 5 and 30% at various ages in surveys over the last 20 years (International Dry Eye Workshop (DEWS) 2007a). Today it is known as a multi-factorial disease of the tears and ocular surface. With potential damage to the ocular surface, DED results in symptoms of discomfort, visual disturbance, and tear film instability (International Dry Eye Workshop (DEWS) 2007b). Patients may complain of burning, itching, stinging, grittiness, foreign body sensation, tearing, ocular fatigue, and dryness. DED is closely associated with increasing age and female gender. In Taiwan, the prevalence of DED is 33.7% in an elderly population. Women get more dry-eye symptoms than men (Lin et al. 2003). DED has significant impact on the quality of life and daily activities (Mertzanis et al. 2005). Currently, the conventional first-line therapy is topical use of artificial tear substitutes which have been found to only relieve symptoms temporarily rather than to treat the underlying cause (Lemp 2008). In order to alleviate these discomforts of DED, new therapies are continuously being explored (Gayton 2009). Although there are increasing studies on this issue, ophthalmologists still suffer from the difficulty of treating moderate-to-severe DED with current treatment options. Moderate-to-severe DED is frequently associated with Sjögren's syndrome or other autoimmune disease (Asbell and Spiegel 2010). Peripheral microvascular damage is one of the characteristics in autoimmune disease. And nail-fold videocapillaroscopy has been used as a tool to recognize the microangiopathy patterns in autoimmune disease (Tektonidou et al. 1999; Ctolo et al. 2004).

Regardless the high potential of Capillaroscopy clinically, there are still some problems needed to be solved. Capillary density, capillary dimensions, blood cell velocity, avascular area, and different capillary patterns are majorly concerned in most studies (Moore et al. 2007; Jones et al. 2002). All the parameters or scores proposed are more or less lacking of quantifying and objective standard for relevancy (Grassi and Angelis 2007). When applying capillaroscopy in practice, an image of good quality is not always presented. Thus image enhancement is crucial for analysis. There have been several image processes proposed to improve quality of the images, such as Laplacian of Gaussian and Skeleton algorithms (Morgan and Payne 2002; Wen et al. 2008). However, a comprehensive and operative system of capillaroscopy is more suitable for clinical practice. There are also a few commercial products for images analysis, such as Cap-Image, CapiScope, JavaCap, Capilab toolbox and AVA 3.0. Most of them are still time-consuming and not ready for everyday clinical use. A reliable,

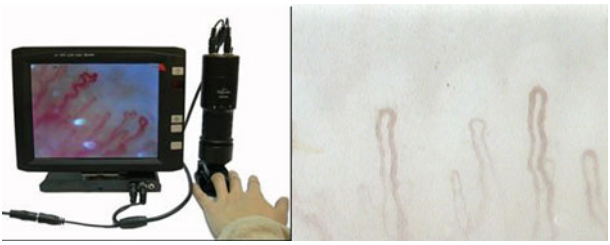

Fig. 1 Model DMX960, capillaroscopy image (640 × 480 pixel)

simple and time-saving computer analyzing program which would increase objectivity is still urgently needed (Anderson et al. 2005; Doherty and Payne 1993; Awan et al. 2010).

This study tries to develop a computerized system of nail-fold capillaroscopy by using a series of algorithms to improve the quality of the images and set up standard measuring procedures, thus the use of nail-fold capillaroscopy could be more accurate and ready for clinical use. This paper is arranged in four parts. The first part introduces a nail-fold capillary related study. The second part presents the detailed description of current work. The third part demonstrates the practical application of the system on normal subjects and DED. The last part states conclusions and future work.

2 Computerized system of nailfold capillaroscopy (CNC)

2.1 Image preparation

2.1.1 Equipment

A nail-fold capillaroscopy image is taken by a microscope coupled with a digital video camera, as shown in Fig. 1 (Model: DMX960, x320, Digilens Co., Taiwan). DMX960 is a portable device with LED light source and a finger holder. The LED light of DMX960 is placed in the surrounding of the lens to avoid any obstruction of the light source. There is also an adjusting filter to control the light reflection of the images. In this way we can have a clear look of the image and gain the most pixels for later calculation. There is a midline marker for identifying the central portion of the tested finger. The images and film are captured by a USB video capture device (Model: UPG304, Upmost Co., Taiwan) with resolution 640 × 480 pixels and stored in a PC for further analysis. The film is taken in a rate of 30 images per second. A pixel is 1.01 μm^2. The area of the visual field is 0.31 mm^2.

2.1.2 Procedures of measurement

The layer of a capillary is only one endothelial cell thick. When the red blood cells pass through these fine capillaries in a single line, the image can be seen clearly and recorded in a single photo or video frames.

All examinations take place in a temperature controlled room ($23-25°C$). The examinees are asked to rest for 15 min before receiving examination. The ring finger of un-dominant hand is the choice on which to perform the examination. The choice of the ring finger can reduce the influence of better microcirculation due to frequent digital movement in daily life (Awan et al. 2010). Mineral oil is applied to the nail-bed of the ring finger to increase visualization. After focus adjustment, one still image and a ten second video film is recorded

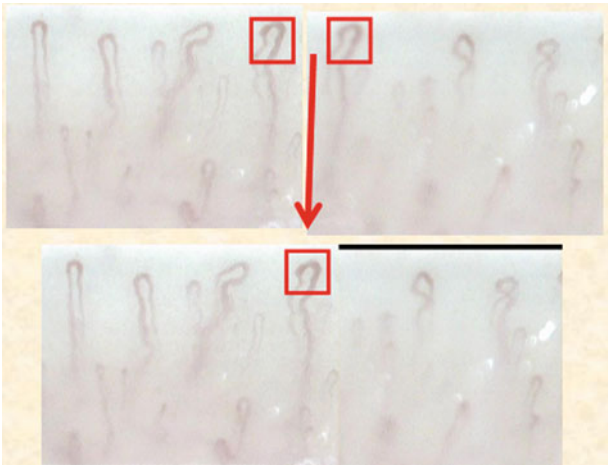

Fig. 2 Composite two images by cross correlation

at the midline of the nail-fold. The distal layer of the capillaries under the papilla is the target portion of the recording. The recording film must include a few functional capillaries with red cells flowing. A series of images (about 9–12 images) are taken from very left to right in a partial overlapping manner to cover the whole nail-fold. The whole examining procedure lasts about 2–5 min. After the examination the result would be classified as good or poor for later analysis reference.

2.2 Panoramic mosaic image and cross correlation

The first step is to produce a composite image of the nail-fold. The image is crucial for evaluation of changes before and after certain intervention (Anderson et al. 2005). Nine to thirteen sequence partial overlapping images from left to right are gained. The registration procedure used two neighbor images each time by Cross correlation until the composite image is complete.

Before proceeding to the Cross correlation, the edges of capillaries need to be enhanced more. A median filter is first applied to the image. The median filter is mainly to reduce noise of the images. It could remove too bright parts and too dark parts of the images. Then a K-means filter divides the image into seven portions by gray scale value. The first four portions turn to black and the rest turn to white. The process is determined by pre-testing. We test many images with different separations beforehand and find that seven portions is most suitable for the image of capillaries. We used K-means to cluster the image in the pretest and got a rather good result both in outcome and operating time. Then a size filter is applied. We tried many images with different size threshold beforehand and found that the threshold of 20% is most suitable for the noise removal. Every sequence image had to undergo the enhancement procedure before connecting to another image.

We make a window of the same pattern on the first and second images. Then we join two images together through calculation of the highest correlation area. The same procedure is repeated until a full composite image is produced. (Figs. 2, 3) The window choice is done manually. It is a simple and time saving procedure for the user. The total process takes about five to ten minutes. We consider it is manageable for a daily task.

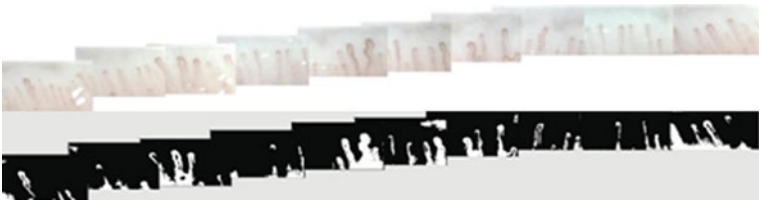

Fig. 3 Panoramic mosaic image for comparison (*upper*: original, *lower*: binary)

Fig. 4 Capillary density by number counting: the capillaries had been diffused to solid-tube shapes and are ready for counting (*lower image*)

2.3 Capillary density by number counting and area percentage

Number counting is defined as number of capillaries per mm^2. Area percentage is defined as total capillary area divided by total area of recorded visual field. In the beginning the quality of image has to be determinate grossly. If the image is good, two kinds of calculations would be performed. If the image is poor, only the density of area percentage would be calculated.

We need to eliminate noise from original image as much as possible to have a clear image for later calculation. A Gaussian filter is first applied to the original image to reduce noise. Then the image is converted to binary and areas of black and white are calculated. White spot area less than 20% of maximum spot was considered as noise and discarded. The decision of the threshold is set by pre-testing. We test many images beforehand to find that the suitable cut for the best differentiation. Next we carry out a morphology operation by highlighting and diffusing the white part of the image, so that the pieces of the same capillary will rejoin together as one solid-tube shape for later counting. We then label the white area and perform the number counting and area percentage calculation. (Figs. 4, 5) The average value of all the images on the panoramic image is presented as capillary density.

2.4 Capillary width

The image taken from the midline portion is used to calculate the width of the capillary unless the quality of the image is too poor. Another clear image would be picked instead. A

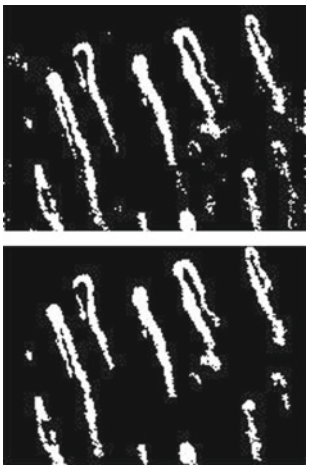

Fig. 5 Capillary density by area percentage: The capillaries had not diffused and were kept in good vessel-like shapes (*lower image*). The accurate percentage of area could be calculated

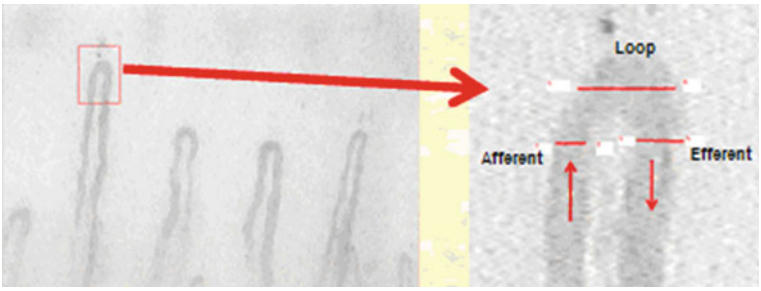

Fig. 6 A clear capillary is picked and enlarged. Afferent, loop and efferent part of capillary are measured

window is selected over the chosen capillary. After enlarging the area the afferent, efferent and loop part are identified and measured manually (Fig. 6). At least three capillaries will be calculated in the image. The average widths are presented as results.

2.5 Blood flow velocity in the capillary

2.5.1 Images generation and shifting control

By transferring the recorded Avi film into series of single images, it generates more than 300 images (the frame rate is 30). Starting from the 110th image to the 200th image, 91 images are selected to avoid any noise of the beginning part. The 110th image is chosen as the basal image. The image rotated and adjusted to make the target capillary vertical for later velocity calculation. All the following images are adjusted in the same manner. During the film recording, some people will have mild finger tremor. It would cause the capillary shifting up and down in the film. We use Cross correlation to control the shifting.

2.5.2 Two double-windows algorithm

We use a Double-windows algorithm to calculate the speed of blood flow (Lin and Lo 2008). A seed point is selected manually inside a vertical capillary of the basal image. Starting from the seed point, 40 pixels and 90 pixels downward, three 10×10 pixels windows (A, B and

C) are generated separately. All the remaining 90 images follow the same rules. The average gray value of each window is calculated.

We use 15 frames as a calculating set. We identify the image R with the maximal average gray value of window A between the 1st image and the 8th image through which a red blood cell first pass. Then we find the image with the maximal value of window B between the image R+2 and image R+4, also we do the same with window C between image R+4 and image R+7. It could represent the same red cell passing through at window B or C. We repeat the rule on window B and C.

The red cell velocity is calculated from the distance of the windows (40, 90 and 50 pixels) and time difference of the frames (1/30 s). Each set we get 3 speeds between A–B, A–C and B–C. We set the range 350–900 to remove unreasonable values from the physiological point of view. The average value of all six groups is presenting as blood velocity.

3 Application of CNC

3.1 Reliability

Before applying CNC to the target subjects, the CNC has to be tested for its reliability. The coefficient of variation (C.V.) is defined as standard deviation (SD) divided by mean. The smaller C.V. shows the better reliability. The inter-capillary and intra-observer variability are tested respectively (Mugii et al. 2009). There is only one operating user in the current study to avoid the differences between different users.

3.1.1 Inter-capillary variability

The variability of capillaries' data is tested on five normal subjects. The coefficients of variation are small which indicates the CNC is reliable to evaluate the microcirculation (Table 1).

3.1.2 Intra-observer variability

The variability is tested in five normal subjects on three separated occasions within 3 weeks. The coefficients of variation are small which indicates the CNC is reliable to evaluate the microcirculation (Table 2).

3.2 Normal subjects and dry eye disease

A total of 36 normal subjects receive capillaroscopy examination according to the procedure proposed. Consent forms are signed. Capillary density, capillary width and blood flow

Table 1 Data of five normal subjects

	Density		Width			Velocity
	Count (N/O.F.)	Area	Afferent (μm)	Efferent (μm)	Loop (μm)	(μm/s)
Mean	6.21	0.13	11.89	13.18	33.79	503.06
SD	1.59	0.01	1.48	1.43	4.20	8.83
C.V.	0.26	0.07	0.12	0.11	0.12	0.02

O.F. stands for "capillaroscopy observation field"

Table 2 Data of five normal subjects on different dates

	Density		Width			Velocity
	Count (N/O.F.)	Area	Afferent (μm)	Efferent (μm)	Loop (μm)	(μm/s)
Mean	6.17	0.15	10.72	11.16	30.68	524.90
SD	1.32	0.02	2.41	2.22	5.30	28.26
C.V.	0.21	0.13	0.22	0.20	0.17	0.05

O.F. stands for "capillaroscopy observation field"

Table 3 Basic data of normal subjects and dry eye disease

	Normal		DED	
Number	36		7	
Gender	Female	Male	Female	Male
	24	12	6	1
Age	57.42 (17.17)		58.33 (18.89)	

Data shows as mean (standard deviation)

Table 4 Capillaroscopy data of normal and DED

	Capillary density		Capillary width (μm)			Blood velocity (μm/s)
	Count (N/O.F.)	Area (%)	Afferent	Efferent	Loop	
Normal	5.58 (1.61)	11.86 (2.87)	9.43 (2.37)	9.67 (2.39)	28.05 (6.27)	530.89 (38.07)
DED	4.12 (1.01)	15.22 (3.97)	12.21 (3.92)	11.47 (2.92)	32 (4.06)	514.57 (24.8)
p value	0.024*	0.016*	0.032*	0.095	0.034	0.127

Data shows as mean (standard deviation). O.F. stands for "capillaroscopy observation field"
* Significant statically

velocity are calculated by CNC. Seven patients of Dry Eye Disease are recruited from the out-patient clinic of the department of Chinese medicine at Changhua Christian hospital. Consent forms are signed as well. There are four patients with Sjögren's syndrome. A total of 43 sets of data are collected. Their descriptive data are presented at Tables 3 and 4. Some images were excluded due to poor quality.

There is no significant difference between the normal group and the DED group in basic data. The Mann-Whitney test was performed to test the statistical differences of capillaroscopy data between two groups, since the data were not normally distributed (Hart 2001). We found density and width of afferent capillary were the better parameters to identify DED. Moreover, there is a trend of reducing tendency in microcirculation of DED by capillary density and blood velocity. The much higher capillary density in area percentage of DED might be due to the malformation of capillary patterns.

4 Conclusion and future work

The study presented a complete solution aiming on the daily clinical use of nail-fold capillaroscopy. It included equipment, measurement procedures, image processing algorithms

and data analyzing methods. A panoramic mosaic image was introduced for comparison of changes. Capillary density, capillary width and blood flow velocity were presented objectively. The total operating time was acceptable and time-saving. A group of 36 normal data was also presented and available for relevant researches. Its clinical application was tested in some DED patients and works well.

The next work would be to develop the pattern recognition part of CNC and to increase the sample size. A new operating user is under training. We will test the reliability among different users in the future. A Double-windows algorithm was used by our colleagues before (Lin and Lo 2008). We made improvement of it and hope to get better results. However, a new technique should be introduced, such as that of Kanade-Lucas Tracker (Zhou et al. 2003), to save time and increase accuracy more. We will try to upgrade this part in our next version. Also the LDA (Ye 2006; Li et al. 2004; Otsu 2005; Shiraki et al. 2006) and SIFT-based recognition process (Kisku et al. 2007; Geng and Jiang 2009) will be introduced in the next version of the system. A discriminant function could be considered to improve the identification of DED.

Acknowledgments We would like to thank Miss Yi-Wei Chao and Mr. Jian-Cheng Chen for their help to collect data.

References

Anderson, M. E., Allen, P. D., Moore, T., Hillier, V., Taylor, C. J., & Herrick, A. L. (2005). Computerized nailfold video capillaroscopy—A new tool for assessment of Raynaud's phenomenon. *The Journal of Rheumatology, 32*(5), 841–848.

Antonios, T. F., Singer, D. R., Markandu, N. D., Mortimer, P. S., & MacGregor, G. A. (1999). Rarefaction of skin capillaries in borderline essential hypertension suggests an early structural abnormality. *Hypertension, 34*(4), 655–658.

Asbell, P. A., & Spiegel, S. (2010). Ophthalmologist perceptions regarding treatment of moderate-to-severe dry eye: Results of a physician survey. *Eye & Contact Lens: Science & Clinical Practice, 36*(1), 33–38.

Awan, Z. A., Wester, T., & Kvernebo, K. (2010). Human microvascular imaging: A review of skin and tongue videomicroscopy techniques and analysing variables. *Clinical Physiology and Functional Imaging, 30*(2), 79–88.

Ctolo, M., Pizzorni, C., Tuccio, M., Burroni, A., Craviotto, C., & Basso, M. (2004). Nailfold videocapillaroscopic patterns and serum autoantibodies in systemic sclerosis. *Rheumatology, 43*, 716–719.

Doherty, A., & Payne, R. R. (1993). Image processing of blurred medical images. In *International conference on acoustic sensing and imaging* (pp. 38–43).

Fagrell, B., Fronek, A., & Intaglietta, M. (1977). A microscope-television system for studying flow velocity in human skin capillaries. *American Journal of Physiology Heart and Circulatory Physiology, 233*(2), H318–321.

Gallucci, F., Russo, R., Buono, R., Acampora, R., Madrid, E., & Uomo, G. (2008). Indications and results of videocapillaroscopy in clinical practice. *Advances in Medical Sciences, 53*(2), 149–157.

Gayton, J. L. (2009). Etiology, prevalence, and treatment of dry eye disease. *Clinical Ophthalmology, 3*, 405–412.

Geng, C., & Jiang, X. (2009). Face recognition using SIFT features. In *2009 16th IEEE international conference on image processing (ICIP)* (pp. 3313–3316).

Grassi, W., & Angelis, R. (2007). Capillaroscopy: questions and answers. *Clinical Rheumatology, 26*(12), 2009–2016.

Hart, A. (2001). Mann-Whitney test is not just a test of medians: Differences in spread can be important. *BMJ, 323*(7309), 391–393.

International Dry Eye Workshop (DEWS). (2007a). The definition and classification of dry eye disease: Report of the Definition and classification subcommittee of the international dry eye workshop. Ocul Surface (Vol. 5, pp. 93–107).

International Dry Eye Workshop (DEWS). (2007b). The definition and classification of dry eye disease: Report of the definition and classification subcommittee of the international dry eye workshop. Ocul Surface (Vol. 5, pp. 75–92).

Jones, B. F., Oral, M., Morris, C. W., & Ring, E. F. J. (2002). A proposed taxonomy for nailfold capillaries based on their morphology. *IEEE Transactions on Medical Imaging, 20*(4), 333–341.

Kisku, D. R., Rattani, A., Grosso, E., & Tistarelli, M. (2007). Face identification by SIFT-based complete graph topology. In *2007 IEEE workshop on automatic identification advanced technologies* (pp. 63–68).

Lambova, S. N., & Müller-Ladner, U. (2009). The specificity of capillaroscopic pattern in connective autoimmune diseases. A comparison with microvascular changes in diseases of social importance: arterial hypertension and diabetes mellitus. *Modern Rheumatology, 19*, 600–605.

Lemp, M. A. (2008). Management of dry eye disease. *The American Journal of Managed Care, 14*(3 suppl), S88–101.

Li, J., Janardan, R., & Li, Q. (2004). Two-dimensional linear discriminant analysis. *Advances in Neural Information Processing Systems, 17*, 1569–1576.

Lin, E. J., & Lo, P. C. (2008). *Analysis of nailfold capillary blood velocity by dual-windows method*. Hsinchu: National Chiao Tung University.

Lin, P. Y., Tsai, S. Y., Cheng, C. Y., Liu, J. H., Chou, P., & Hsu, W. M. (2003). Prevalence of dry eye among an elderly Chinese population in Taiwan: The Shihpai eye study. *Ophthalmology, 110*, 1096–1101.

Mertzanis, P., Abetz, L., Rajagopalan, K., Espindle, D., Chalmers, R., Snyder, C., & Caffery, B. (2005). The relative burden of dry eye in patients' lives: Comparisons to a US normative sample. *Investigative Ophthalmology & Visual Science, 46*(1), 46–50.

Moore, T. L., Vail, A., & Herrick, A. L. (2007). Assessment of digital vascular structure and function in response to bosentan in patients with systemic sclerosis-related Raynaud's phenomenon. *Rheumatology, 46*(2), 363–373.

Morgan, T. P., & Payne, R. R. (2002). The deblurrinq of medical images. In *IEE Colloquium on medical imaging: Image processing and analysis* (pp. 2/1–2/5).

Mugii, N., Hasegawa, M., Hamaguchi, Y., Tanaka, C., Kaji, K., & Komura, K. (2009). Reduced red blood cell velocity in nail-fold capillaries as a sensitive and specific indicator of microcirculation injury in systemic sclerosis. *Rheumatology, 48*(6), 696–703.

Otsu, N. (2005). Towards flexible and intelligent vision systems-from thresholding to CHLAC. In *Proceedings of IAPR conference on machine vision applications* (pp. 430–439).

Shiraki, T., Saito, H., Kamoshida, Y., Ishiguro, K., Fukano, R., & Shirai, T., et al. (2006). Real-Time motion recognition using chlac features and cluster computing. In *Proceedings of the 3rd IFIP international conference on network and parallel computing* (pp. 50–56).

Tektonidou, M., Kaskani, E., Skopouli, F. N., & Moutsopoulos, H. M. (1999). Microvascular abnormalities in Sjögren's syndrome: Nailfold capillaroscopy. *Rheumatology, 38*, 826–830.

Wen, C. H., Hsieh T. Y., Liao, W. D., Lan, J. L., Chen, D. Y., & Li, K. C., et al. (2008). A novel method for classification of high-resolution nailfold capillary microscopy images. In *First IEEE international conference on ubi-media computing* (pp. 513–518).

Ye, J. (2006). Characterization of a family of algorithms for generalized discriminant analysis on undersampled problems. *Journal of Machine Learning Research, 6*(1), 483–502.

Zhou, X., Collins, R. T., Kanade, T., & Metes, P. (2003). A master-slave system to acquire biometric imagery of humans at distance. In *First ACM SIGMM international workshop on video surveillance* (pp. 113–120).